



Cite this: *Chem. Commun.*, 2015, 51, 4425

Received 19th January 2015,  
Accepted 6th February 2015

DOI: 10.1039/c5cc00529a

www.rsc.org/chemcomm

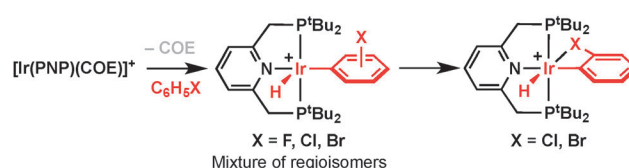
# Low-coordinate iridium NHC complexes derived from selective and reversible C–H bond activation of fluoroarenes†

Simone A. Hauser, Ivan Prokes and Adrian B. Chaplin\*

**Interaction of the reactive 14 VE  $\{\text{Ir}(\text{IBioxMe}_4)_3\}^+$  fragment with fluoroarenes results exclusively in *ortho*-C–H bond oxidative addition and formation of 16 VE Ir(III) derivatives  $[\text{Ir}(\text{IBioxMe}_4)_3(\text{Ar})\text{H}]^+$  ( $\text{Ar} = 2\text{-C}_6\text{H}_4\text{F}$ ,  $2,3\text{-C}_6\text{H}_3\text{F}_2$ ,  $2,4,6\text{-C}_6\text{H}_2\text{F}_3$ ). The C–H bond activation reactions occur under mild conditions and are reversible.**

The transition-metal-mediated C–H bond activation of partially fluorinated arenes is a potentially powerful means for accessing aryl fluoride synthons in organic chemistry,<sup>1,2</sup> providing an orthogonal synthetic strategy to aryl C–F bond functionalisation and late stage aromatic fluorination protocols.<sup>3,4</sup> Supporting the development of this methodology, an increasing number of transition metal systems capable of C–H bond activation of simple aryl fluorides are being described.<sup>5,6</sup> Systems involving well defined and electronically unsaturated metal–aryl products are of particular interest as catalyst models, although examples remain scarce.<sup>7</sup> As a latent source of a highly reactive 14 VE Ir(I) fragment,  $[\text{Ir}(\text{PNP})(\text{COE})]^+$  (COE = cyclooctene; PNP =  $2,6\text{-(P}^t\text{Bu}_2\text{CH}_2)_2\text{-C}_5\text{H}_3\text{N}$ ) is particularly notable in this regard, undergoing C–H bond oxidative addition of fluorobenzene following dissociation of COE (Scheme 1).<sup>8</sup> The reaction however lacks regioselectivity; selectivity that can be induced in analogous reactions with chloro- and bromo-benzene, through chelation of the halide to the metal. Similar chemistry is observed for the related neutral iridium fragment  $\{\text{Ir}(\text{PNP}^*)\}$  (PNP\* =  $(2\text{-P}^t\text{Bu}_2\text{-4-MeC}_6\text{H}_3)_2\text{N}^-$ ), although thermolysis ultimately results in C–X bond activation with PhCl and PhBr.<sup>9</sup>

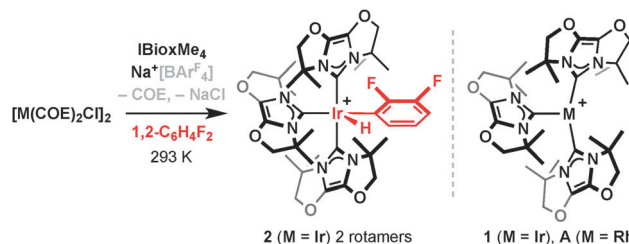
As part of our ongoing work investigating the coordination chemistry of Glorius' bioxazoline derived NHC ligand IBioxMe<sub>4</sub>,<sup>10</sup> we describe here an iridium system which is capable of selectively activating the C–H bonds of fluoroarenes under mild conditions



**Scheme 1** C–H bond activation of aryl halides using an iridium pincer complex.

and leads to electronically unsaturated 16 VE aryl hydride products. Drawing upon the conformationally rigid geometry to attenuate ligand cyclometalation, IBioxMe<sub>4</sub> has previously enabled the isolation of  $[\text{Rh}(\text{IBioxMe}_4)_3][\text{BAR}^{\text{F}}_4]$  (**A**, Scheme 2;  $\text{Ar}^{\text{F}} = 3,5\text{-C}_6\text{H}_3(\text{CF}_3)_2$ ).<sup>11</sup> Formally 14 VE, **A** is notable for the absence of any significant stabilising agostic interactions and complete solution stability ( $\text{CH}_2\text{Cl}_2$ ,  $1,2\text{-C}_6\text{H}_4\text{F}_2$ ). Targeting preparation of the iridium analogue **1**, we reacted  $[\text{Ir}(\text{COE})_2\text{Cl}]_2$  with IBioxMe<sub>4</sub> in  $1,2\text{-C}_6\text{H}_4\text{F}_2$  in the presence of  $\text{Na}[\text{BAR}^{\text{F}}_4]$  as a halide abstractor (293 K). Resulting instead in activation of the solvent, Ir(III) derivative  $[\text{Ir}(\text{IBioxMe}_4)_3(2,3\text{-C}_6\text{H}_3\text{F}_2)\text{H}][\text{BAR}^{\text{F}}_4]$  (**2**) was exclusively observed and subsequently isolated in high yield as an ~1 : 1 mixture of rotamers (76%). The selective formation of an *ortho*-activated derivative is in line with previous work that has established a strong electronic preference for C–H bond activation adjacent to fluorine substituents.<sup>1</sup>

The formation of **2** is characterised by the presence of two sharp and very low frequency <sup>1</sup>H resonances at  $\delta -47.09$  and



**Scheme 2** Preparation of tris-IBioxMe<sub>4</sub> complexes of iridium and rhodium.  $[\text{BAR}^{\text{F}}_4]^-$  anions omitted for clarity.

Department of Chemistry, University of Warwick, Gibbet Hill Road, Coventry CV4 7AL, UK. E-mail: a.b.chaplin@warwick.ac.uk;

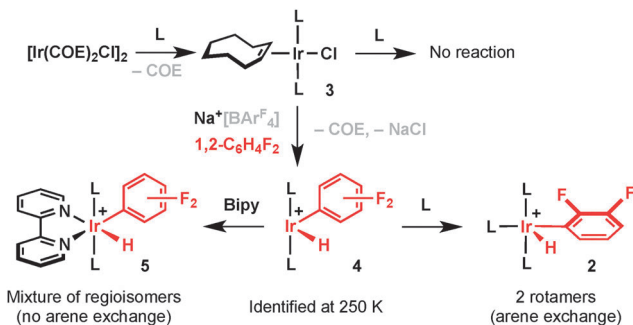
Web: <http://go.warwick.ac.uk/abchaplin>, [www.twitter.com/chapinlab](http://www.twitter.com/chapinlab)

† Electronic supplementary information (ESI) available: Full experimental details and selected NMR spectra. CCDC 1037606 (**2**), 1037607 (**5**), 1037610 (**6**), 1037611 (**7**) and 1037618 (**8**). For ESI and crystallographic data in CIF or other electronic format see DOI: 10.1039/c5cc00529a



–48.67, for each of the rotamers respectively, typical of species bearing hydride ligands *trans* to a vacant coordination site.<sup>12</sup> The former hydride resonance shows a through space  $^1\text{H}_{\text{FH}}$  coupling of 3.7 Hz, identifying it as rotamer of **2** with the hydride and aryl fluoride groups *syn* with respect to the metal–aryl bond (as depicted in Scheme 2). Two sets of multiple coupled resonances at  $\delta$  –111.6/–139.4 ( $^3J_{\text{FF}} = 27$  Hz) and –114.9/–139.9 ( $^3J_{\text{FF}} = 28$  Hz) are likewise observed in the  $^{19}\text{F}\{^1\text{H}\}$  NMR spectrum ( $\text{CD}_2\text{Cl}_2$ ). The former pair are ascribed to the *syn*-rotamer as the resonance at  $\delta$  –111.6 shows  $^1\text{H}_{\text{FH}}$  coupling. The characterisation of **2** in solution is complemented in the solid-state by X-ray diffraction: one of the two independent, but structurally similar, cations of **2** is shown in Fig. 1. The rotamers cannot be distinguished due to disorder of the aryl ligands about the metal–aryl bond and the inability to locate the hydride ligands on the difference Fourier map. The 2-fluorine substituents notably remain significantly distant from the metal centre in **2** ( $\text{Ir} \cdots \text{F} > 3.2$  Å) and two methyl substituents of the IBioxMe<sub>4</sub> ligands adopt strong  $\text{CH} \cdots \pi$  interactions with the aryl ligand (*ca.* 2.3–2.7 Å); an interaction that is manifested in the  $^1\text{H}$  NMR spectrum by distinctly shielded methyl resonances ( $\delta$  0.15–0.28).

To help elucidate the underlying mechanism, we have investigated the reaction step-wise in 1,2- $\text{C}_6\text{H}_4\text{F}_2$  (Scheme 3). Starting with  $[\text{Ir}(\text{COE})_2\text{Cl}]_2$ , addition of excess IBioxMe<sub>4</sub> resulted in rapid (<10 min) and quantitative formation of *trans*- $[\text{Ir}(\text{IBioxMe}_4)_2(\text{COE})\text{Cl}]$  (**3**), which retains the coordinated hydrocarbon ligand even on heating in the presence of IBioxMe<sub>4</sub> (3 h, 333 K). Analogous iridium complexes containing less sterically imposing NHC ligands than IBioxMe<sub>4</sub> ( $\%V_{\text{bur}} = 32\%$ ) have previously been prepared under similar conditions.<sup>13</sup> Interaction of  $[\text{Ir}(\text{COE})_2\text{Cl}]_2$  with more comparably sized ligands, however, is known to result in cyclo-metallation of the NHC, *e.g.* IMes (1,3-bis-mesitylimidazol-2-ylidene;  $\%V_{\text{bur}} = 32\%$ ), IPr (1,3-bis(2,6-diisopropylphenyl)imidazol-2-ylidene;  $\%V_{\text{bur}} = 34\%$ ) and *t*Bu (1,3-bis-*tert*-butylimidazol-2-ylidene;  $\%V_{\text{bur}} = 36\%$ ).<sup>14,15</sup> The formation and stability of **3**, therefore reinforces the ability to partner IBioxMe<sub>4</sub> with reactive metal centres without intramolecular activation.<sup>11</sup> Reaction of isolated **3** with



**Scheme 3** Mechanistic investigations into the formation of **2** (L = IBioxMe<sub>4</sub>). Reactions in 1,2- $\text{C}_6\text{H}_4\text{F}_2$  at 293 K unless otherwise indicated.  $[\text{BARF}_4]^-$  anions omitted for clarity.

1.1 equivalents of  $\text{Na}[\text{BARF}_4]$  at 250 K resulted in the rapid liberation of COE (<10 min) and formation of an unstable hydride species **4** as the major organometallic species (*ca.* 80%). The formation of **4** is characterised by the presence of four low frequency hydride signals at  $\delta$  –44.91, –46.37, –46.48 and –46.61 of similar intensity alongside multiple sets of coupled signals in the  $^{19}\text{F}$  NMR spectrum, suggesting unselective C–H bond oxidative addition of 1,2- $\text{C}_6\text{H}_4\text{F}_2$ . The formulation of **4** as 14 VE Ir(III) aryl hydride has structural precedence in the electronically similar dihydride  $[\text{Ir}(\text{tBu})_2(\text{H})_2]^+{}^{15d}$ .

As complex **4** proved intractable to further isolation, we instead sought to gain additional insight by studying its reactivity *in situ* with bipyridine and IBioxMe<sub>4</sub>. Consistent with **4** being a kinetically viable intermediate in the formation of **2** from  $[\text{Ir}(\text{COE})_2\text{Cl}]_2$ , reaction with IBioxMe<sub>4</sub> resulted in quantitative formation of **2** – containing solely an *ortho*-C–H bond activated difluorobenzene. Indeed **2** is conveniently prepared directly from **3**, IBioxMe<sub>4</sub> and  $\text{Na}[\text{BARF}_4]$  in 1,2- $\text{C}_6\text{H}_4\text{F}_2$  with an isolated yield of 74%. Reacting **4** instead with 2,2'-bipyridine led to complete conversion into 18 VE Ir(III) complex **5**, which was ultimately isolated in 82% yield. This new complex is stable in  $\text{CD}_2\text{Cl}_2$  and obtained as a ~1.2 : 1 mixture of *ortho*- and *meta*-difluorobenzene activation products, which in contrast to **2** shows restricted rotation about the metal–aryl bond on the

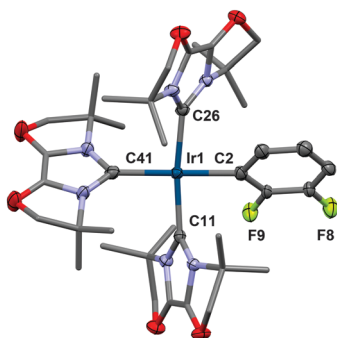


**Fig. 1** Solid-state structure of **2** ( $Z' = 2$ ). Thermal ellipsoids at 50% probability level for selected atoms; minor disordered components, hydrogen atoms, anions and solvent molecule omitted for clarity. Selected bond lengths [Å] and angles [°]: Ir1–C2, 2.090(4); Ir1–C11, 2.072(4); Ir1–C26, 2.097(4); Ir1–C41, 2.113(4); C2–Ir1–C41, 179.46(14); C11–Ir1–C26, 171.72(16); Ir2–C102, 2.094(2).

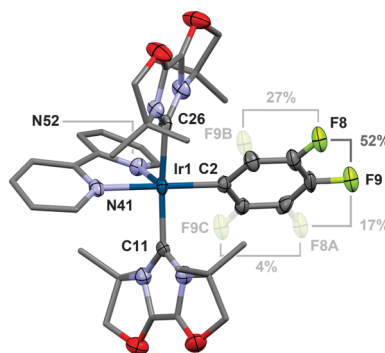
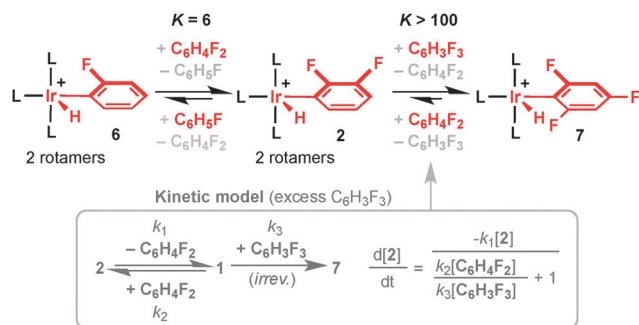


**Fig. 2** Solid-state structure of **5**. Thermal ellipsoids at 50% probability level for selected atoms; hydrogen atoms, anion and solvent molecule omitted for clarity. Selected bond lengths [Å] and angles [°]: Ir1–C2, 2.053(6); Ir1–C11, 2.062(6); Ir1–C26, 2.093(7); Ir1–N41, 2.134(5); Ir1–N52, 2.204(5); C2–Ir1–N41, 175.4(2); C11–Ir1–C26, 168.5(2).





**Scheme 4** Arene exchange reactions ( $\text{L} = \text{IBioxMe}_4$ ). Measured at 298 K.  $[\text{BAR}^{\text{F}}_4]^-$  anions omitted for clarity.

NMR time scale (500 MHz). The dynamic processes are frozen out on cooling in  $\text{CD}_2\text{Cl}_2$ , however decoalescence for the 2,3-regioisomer occurs at significantly higher temperature (273 K,  $\Delta G^\ddagger \sim 57 \text{ kJ mol}^{-1}$ ) compared to the 3,4-regioisomer (200 K,  $\Delta G^\ddagger \sim 46 \text{ kJ mol}^{-1}$ ). The presence of isomers is also apparent in the solid-state structure, which crystallises as a mixture of regioisomers and their respective rotamers (Fig. 2).<sup>16</sup>

The reactions of **4** suggest that the high regioselectivity observed in the formation of **2** is thermodynamic in origin, invoking reversible C–H bond activation and the transient presence of **1**. This hypothesis is supported by the previous isolation of **A** and equilibrium reactions of **2** with fluoroarene and 1,3,5-trifluorobenzene that result in the reversible formation of **6** (exclusively 2-regioisomer) and **7**, respectively (monitored by  $^1\text{H}$  and  $^{19}\text{F}$  NMR spectroscopy, Scheme 4). The formulation of these new Ir(III) complexes was verified by independent synthesis from **3**,  $\text{IBioxMe}_4$  and  $\text{Na}[\text{BAR}^{\text{F}}_4]$  in the appropriate fluoroarene, with isolated yields of 66% and 80% for **6** and **7**, respectively. Both complexes were fully characterised in solution and the solid-state and share similar structural characteristics with **2** (see ESI† and Fig. 3). Notably no arene exchange is observed for **5**, suggesting the interaction of **4** with 2,2'-bipyridine has captured a mixture of kinetic products of fluoroarene activation on halide extraction from **3**. Consistent with previous findings that M–C bond strength increases with F substitution,<sup>1</sup> the equilibrium reactions clearly indicate more favourable oxidative addition in the order  $\text{C}_6\text{H}_5\text{F} < 1,2\text{-C}_6\text{H}_4\text{F}_2 \ll 1,3,5\text{-C}_6\text{H}_3\text{F}_3$ .

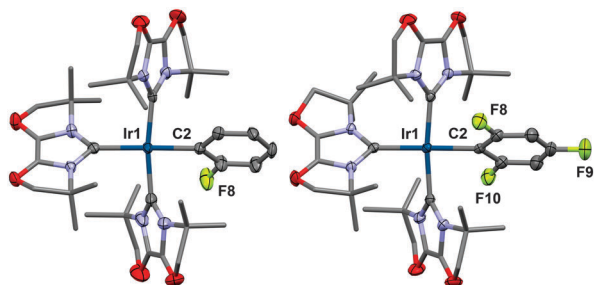


**Fig. 3** Solid-state structures of **6** (left) **7** (right,  $Z' = 2$ ). Thermal ellipsoids at 50% probability level for selected atoms; hydrogen atoms, anions and solvent molecule (**6**) omitted for clarity. Selected bond lengths [Å]: **6**: Ir1–C2, 2.066(5); **7**: Ir1–C2, 2.092(3).

To help substantiate the transient presence of **1** in the C–H bond activation processes, we have probed the kinetics for the formation of **7** from **2** and 1,3,5-trifluorobenzene. Measuring the rate of this reaction using five different solvent mixtures of  $[1,2\text{-C}_6\text{H}_4\text{F}_2]$  and  $[1,3,5\text{-C}_6\text{H}_3\text{F}_3]$  ( $\geq 50 \text{ equiv./2}$ ) enabled us to establish a two-step kinetic model for the arene exchange, involving pre-equilibrium formation of **1** by reductive elimination of 1,2-difluorobenzene ( $R^2 = 0.998$  for fit, Scheme 4). Under this kinetic model, the rate of reductive elimination ( $k_1$ ) was determined to be  $(1.5 \pm 0.9) \times 10^{-3} \text{ s}^{-1}$  at 298 K. For comparison, we have also estimated the rate of reductive elimination of 1,3,5-trifluorobenzene at 298 K ( $(1.96 \pm 0.15) \times 10^{-6} \text{ s}^{-1}$ ) by dissolving **7** in pure 1,2-difluorobenzene, and measuring the initial rate of the ensuing reaction. Arene exchange is much faster for **6** in 1,2-difluorobenzene at 298 K ( $< 10 \text{ min}$ ), corresponding to a lower bound for the rate of fluoroarene reductive elimination at 298 K of  $3 \times 10^{-3} \text{ s}^{-1}$ .

In view of the facile elimination of fluoroarene apparent from the aforementioned arene exchange reactions, we have also attempted to isolate **1** by dissolving **6** in perfluorotoluene at 293 K, but with limited success. Analysis by  $^1\text{H}$  NMR spectroscopy indicated the liberation of fluoroarene into solution and the transient presence of a cationic tris-ligated  $\text{IBioxMe}_4$  species of high symmetry. The poor solubility and extremely high apparent reactivity of this species, however, has so far proven prohibitive to isolation and any further interrogation. Instead, we proceeded to trap out **1** using a strongly coordinating solvent. Dissolving **2**, **6** and **7** in MeCN, resulted in reductive elimination of fluoroarene and formation of the acetonitrile adduct of **1**,  $[\text{Ir}(\text{IBioxMe}_4)_3(\text{NCMe})][\text{BAR}^{\text{F}}_4]$  (**8**), in each case (Fig. 4). The rates for this reaction measured *in situ* by  $^{19}\text{F}$  NMR spectroscopy parallel those determined for the arene exchange reactions, although they are all slower presumably as a consequence of non-negligible coordination of MeCN to the aryl hydride precursors ( $(2.7 \pm 0.3) \times 10^{-3} \text{ s}^{-1}$ , **6**;  $(0.120 \pm 0.007) \times 10^{-3} \text{ s}^{-1}$ , **2**;  $(3.84 \pm 0.13) \times 10^{-7} \text{ s}^{-1}$ , **7**; all at 298 K).<sup>17</sup> In the case of **2**, complex **8** was isolated in 87% yield (Fig. 4). In MeCN solution the reductive elimination of fluoroarene is to all intents and purposes irreversible. Successively dissolving **8** in 1,2- $\text{C}_6\text{H}_4\text{F}_2$  and removing the solvent *in vacuo*, however, does eventually lead to the partial reformation of **2** (70% conversion after 7 cycles).

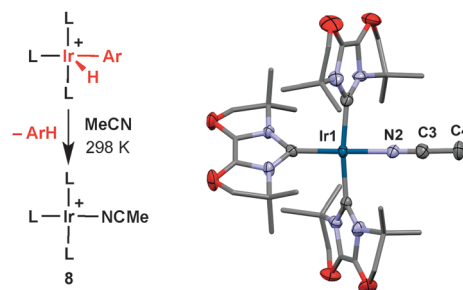


**Fig. 4** Preparation and solid-state structure of **8**. In scheme:  $\text{L} = \text{IBioxMe}_4$ ;  $\text{Ar} = 2\text{-C}_6\text{H}_4\text{F}$ ,  $2,3\text{-C}_6\text{H}_3\text{F}_2$ ,  $2,4,6\text{-C}_6\text{H}_2\text{F}_3$ ;  $[\text{BAR}^{\text{F}}_4]^-$  anions omitted for clarity. In solid-state structure: thermal ellipsoids at 50% probability level for selected atoms; hydrogen atoms and anion omitted for clarity.

In summary, we have demonstrated that both bis-NHC and tris-NHC ligated Ir(I) species are capable of C–H bond oxidative addition of fluoroarene substrates under mild conditions, however it is only with the three coordinate  $\{\text{Ir}(\text{IBioxMe}_4)_3\}^+$  fragment that regioselectivity is achieved. The formation of *ortho*-activated products is in line with previous work purporting the electronic preference for activation at these positions and enabled through reaction reversibility.<sup>1</sup> In view of related work using PNP and PNP\* pincer scaffolds,<sup>8,9</sup> it is evident that 14 VE Ir(I) fragments are well suited for C–H bond activation reactions of fluorinated aromatics, although their reactivity must be moderated in order to favour the formation of thermodynamic rather than kinetic activation products. Conformationally rigid IBioxMe<sub>4</sub> ligands appear to be well suited to this purpose, combining resistance to intramolecular C–H bond activation with strong  $\sigma$ -donor and *trans*-influence characteristics. We are currently engaged in investigating ways in which such design principles can be applied in catalysis.

We gratefully acknowledge financial support from the Swiss National Science Foundation (S.A.H.), Royal Society (A.B.C) and University of Warwick. Crystallographic data was collected using a diffractometer purchased through support from Advantage West Midlands and the European Regional Development Fund.

## Notes and references

- 1 E. Clot, O. Eisenstein, N. Jasim, S. A. Macgregor, J. E. McGrady and R. N. Perutz, *Acc. Chem. Res.*, 2011, **44**, 333–348.
- 2 (a) X. C. Cambeiro, T. C. Boorman, P. Lu and I. Larrosa, *Angew. Chem., Int. Ed.*, 2012, **52**, 1781–1784; (b) Y. Nakao, N. Kashiwara, K. S. Kanyiva and T. Hiyama, *J. Am. Chem. Soc.*, 2008, **130**, 16170–16171; (c) H.-Q. Do and O. Daugulis, *J. Am. Chem. Soc.*, 2008, **130**, 1128–1129; (d) M. Lafrance, C. N. Rowley, T. K. Woo and K. Fagnou, *J. Am. Chem. Soc.*, 2006, **128**, 8754–8756.
- 3 (a) T. Ahrens, J. Kohlmann, M. Ahrens and T. Braun, *Chem. Rev.*, 2015, **115**, 931–972; (b) M. K. Whittlesey and E. Peris, *ACS Catal.*, 2014, **4**, 3152–3159; (c) M. F. Kuehnle, D. Lentz and T. Braun, *Angew. Chem., Int. Ed.*, 2013, **52**, 3328–3348.
- 4 (a) T. Liang, C. N. Neumann and T. Ritter, *Angew. Chem., Int. Ed.*, 2013, **52**, 8214–8264; (b) T. Furuya, A. S. Kamlet and T. Ritter, *Nature*, 2012, **473**, 470–477; (c) D. A. Watson, M. Su, G. Teverovskiy, Y. Zhang, J. Garcia-Fortanet, T. Kinzel and S. L. Buchwald, *Science*, 2009, **325**, 1661–1664; (d) J. M. Brown and V. Gouverneur, *Angew. Chem., Int. Ed.*, 2009, **48**, 8610–8614.
- 5 (a) M. E. Evans, C. L. Burke, S. Yaibuathes, E. Clot, O. Eisenstein and W. D. Jones, *J. Am. Chem. Soc.*, 2009, **131**, 13464–13473; (b) A. D. Selmecky, W. D. Jones, M. G. Partridge and R. N. Perutz, *Organometallics*, 1994, **13**, 522–532.
- 6 (a) A. S. Romanov and M. Bochmann, *Organometallics*, 2015, DOI: 10.1021/om501211p; (b) J. C. DeMott, N. Bhuvanesh and O. V. Ozerov, *Chem. Sci.*, 2013, **4**, 642–649; (c) P. Lu, T. C. Boorman, A. M. Z. Slawin and I. Larrosa, *J. Am. Chem. Soc.*, 2010, **132**, 5580–5581; (d) B. C. Bailey, J. C. Huffman and D. J. Mindiola, *J. Am. Chem. Soc.*, 2007, **129**, 5302–5303; (e) E. Clot, M. Besora, F. Maseras, C. Mègret, O. Eisenstein, B. Oelckers and R. N. Perutz, *Chem. Commun.*, 2003, 490–491; (f) J. J. Carbó, O. Eisenstein, C. L. Higgit, A. H. Klahn, F. Maseras, B. Oelckers and R. N. Perutz, *J. Chem. Soc., Dalton Trans.*, 2001, 1452–1461; (g) F. Godoy, C. L. Higgit, A. H. Klahn, B. Oelckers, S. Parsons and R. N. Perutz, *J. Chem. Soc., Dalton Trans.*, 1999, 2039–2048; (h) J. Forniés, M. Green, J. L. Spencer and F. G. A. Stone, *J. Chem. Soc., Dalton Trans.*, 1977, 1006–1009.
- 7 (a) K. B. Renkema, R. Bosque, W. E. Streib, F. Maseras, O. Eisenstein and K. G. Caulton, *J. Am. Chem. Soc.*, 1999, **121**, 10895–10907; (b) R. Bosque, E. Clot, S. Fantacci, F. Maseras, O. Eisenstein, R. N. Perutz, K. B. Renkema and K. G. Caulton, *J. Am. Chem. Soc.*, 1998, **120**, 12634–12640.
- 8 (a) E. Ben-Ari, R. Cohen, M. Gandelman, L. J. W. Shimon, J. M. L. Martin and D. Milstein, *Organometallics*, 2006, **25**, 3190–3210; (b) E. Ben-Ari, M. Gandelman, H. Rozenberg, L. J. W. Shimon and D. Milstein, *J. Am. Chem. Soc.*, 2003, **125**, 4714–4715.
- 9 The regioselectivity of the C–H bond activation of PhF is not discussed in great detail, except that the number of isomers changes on thermolysis. L. Fan, S. Parkin and O. V. Ozerov, *J. Am. Chem. Soc.*, 2005, **127**, 16772–16773.
- 10 G. Altenhoff, R. Goddard, C. W. Lehmann and F. Glorius, *J. Am. Chem. Soc.*, 2004, **126**, 15195–15201.
- 11 (a) A. B. Chaplin, *Organometallics*, 2014, **33**, 3069–3077; (b) A. B. Chaplin, *Organometallics*, 2014, **33**, 624–626.
- 12 P. S. Pregosin, *NMR in Organometallic Chemistry*, Wiley-VCH, Weinheim, 2012.
- 13 D. J. Nelson, B. J. Truscott, A. M. Z. Slawin and S. P. Nolan, *Inorg. Chem.*, 2013, **52**, 12674–12681.
- 14 A. Poater, B. Cosenza, A. Correa, S. Giudice, F. Ragone, V. Scarano and L. Cavallo, *Eur. J. Inorg. Chem.*, 2009, 1759–1766.
- 15 (a) C. Y. Tang, W. Smith, A. L. Thompson, D. Vidovic and S. Aldridge, *Angew. Chem., Int. Ed.*, 2010, **50**, 1359–1362; (b) C. Y. Tang, W. Smith, D. Vidovic, A. L. Thompson, A. B. Chaplin and S. Aldridge, *Organometallics*, 2009, **28**, 3059–3066; (c) N. M. Scott, R. Dorta, E. D. Stevens, A. Correa, L. Cavallo and S. P. Nolan, *J. Am. Chem. Soc.*, 2005, **127**, 3516–3526; (d) N. M. Scott, V. Pons, E. D. Stevens, D. M. Heinekey and S. P. Nolan, *Angew. Chem., Int. Ed.*, 2005, **44**, 2512–2515.
- 16 Refinement of the aryl substituents yields different isomer ratios to those observed in solution, presumably resulting from subtly different crystal packing effects and crystallisation kinetics of the isomers.
- 17 Supporting the suggestion of reversible interaction of MeCN with the aryl hydride complexes, line broadening of the hydride resonance(s) is/are observed in d<sub>3</sub>-MeCN at 298 K.

